

Complexation of Fluorosurfactants to Functionalized Solid Surfaces: Smart Behavior

S. J. Hutton, J. M. Crowther, and J. P. S. Badyal*

Department of Chemistry, Science Laboratories, Durham University,
Durham DH1 3LE, England, U.K.

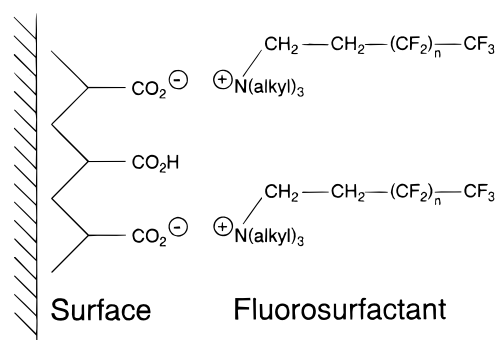
Received February 10, 2000. Revised Manuscript Received May 24, 2000

Complexation of cationic fluorosurfactants to well-defined acrylic acid plasma polymer surfaces gives rise to oleophobic/hydrophilic behavior. This is in marked contrast to the usual oleophobic/hydrophobic liquid repellent attributes of conventional polyelectrolyte–fluorosurfactant complexes formed by solution-phase synthesis.

Introduction

Polyelectrolytes can spontaneously interact with oppositely charged surfactants in aqueous solution to produce polyelectrolyte–surfactant complexes according to a strict 1:1 stoichiometry required for overall charge balance.^{1–3} These systems have been extensively studied in the past as a function of many parameters including surfactant tail length,^{4–9} nature of the polyelectrolyte,^{8–13} density of charge sites along the polyelectrolyte backbone,^{5,11,12,14,15} solution pH,⁸ and the incorporation of low molecular weight electrolyte.^{4,5,8,15–18} A combination of electrostatic attraction between the oppositely charged constituents and interactions between the long-chain surfactant tails is understood to culminate in a highly cooperative binding process, which leads to stabilization of the polyelectrolyte–surfactant complex.^{4,5,16,17,19–23} In

Scheme 1. Complexation between the Plasma Polymer Surface and Cationic Fluorosurfactant



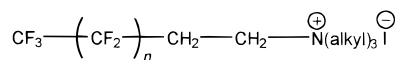
the solid phase, these materials tend to display a layered arrangement derived from demixing of the polar polyelectrolyte backbone and the hydrophobic surfactant tails. The precise structure is influenced by a number of factors which include the relative volume fractions of ionic and alkyl phases present, and the molecular geometry of the surfactant molecules.¹ In fact polyelectrolyte–surfactant complexes with cubic, lamellar, and cylindrical morphologies have been observed.^{1–3} These materials are of technological importance; for example, polyelectrolyte–fluorosurfactant complexes²⁴ are being considered for ultralow surface energy applications, such as water-repellent fabrics, self-lubricating machine parts, and other nonstick end uses.

Conventionally the whole polyelectrolyte–surfactant complex is prepared in solution, precipitated, and then applied to a substrate. In this paper, a more direct approach is outlined comprising the coupling of ionic surfactants to predeposited polyelectrolyte plasma polymer surfaces, Scheme 1. Plasma polymerization is attractive from the perspective that a wide range of substrate materials can be coated irrespective of their chemical nature, shape, or topography.^{25,26} Complexation of a cationic fluorosurfactant (a trialkylammonium

- * To whom correspondence should be addressed.
- (1) Antonietti, M.; Burger, C.; Conrad, J.; Kaul, A. *Macromol. Symp.* **1996**, *106*, 1.
 - (2) Antonietti, M.; Conrad, J.; Thünemann, A. *Macromolecules* **1994**, *27*, 6007.
 - (3) Antonietti, M.; Burger, C.; Effing, J. *Adv. Mater.* **1995**, *7*, 751.
 - (4) Goddard, E. D. *Colloids Surf.* **1986**, *19*, 301.
 - (5) Lindman, B.; Thalberg, K. In *Interactions of Surfactants with Polymers and Proteins*; Goddard, E. D., Ananthapadmanabhan, K. P., Eds.; CRC: Boca Raton, FL, 1993; Chapter 5.
 - (6) Okuzaki, H.; Osada, Y. *Macromolecules* **1994**, *27*, 502.
 - (7) Okuzaki, H.; Eguchi, Y.; Osada, Y. *Chem. Mater.* **1994**, *6*, 1651.
 - (8) Zezin, A. B.; Izumrudov, V. A.; Kabanov, V. A. *Macromol. Symp.* **1996**, *106*, 397.
 - (9) Thalberg, K.; Lindman, B.; Karlström, G. *J. Phys. Chem.* **1991**, *95*, 3370.
 - (10) Shimizu, T.; Seki, M.; Kwak, J. C. T. *Colloids Surf.* **1986**, *20*, 289.
 - (11) Shimizu, T. *Colloids Surf., A* **1995**, *94*, 115.
 - (12) Okuzaki, H.; Osada, Y. *Macromolecules* **1995**, *28*, 4554.
 - (13) Macdonald, P. M.; Tang, A. *Langmuir* **1997**, *13*, 2259.
 - (14) Fundin, J.; Hansson, P.; Brown, W.; Lidegran, I. *Macromolecules* **1997**, *30*, 1118.
 - (15) Thalberg, K.; Lindman, B.; Bergfeldt, K. *Langmuir* **1991**, *7*, 2893.
 - (16) Hayakawa, K.; Kwak, J. C. T. Chapter 5. In *Cationic Surfactants, Physical Chemistry*; Rubingh, D. N., Holland, P. M., Eds.; Marcel Dekker: New York, 1991; p 189.
 - (17) Hayakawa, K.; Kwak, J. C. T. *J. Phys. Chem.* **1982**, *86*, 3866.
 - (18) Herslöf, Å.; Sundelöf, L.-O.; Edsman, K. *J. Phys. Chem.* **1992**, *96*, 2345.
 - (19) Hayakawa, K.; Kwak, J. C. T. *J. Phys. Chem.* **1983**, *87*, 506.
 - (20) Hayakawa, K.; Santerre, J. P.; Kwak, J. C. T. *Macromolecules* **1983**, *16*, 1642.
 - (21) Santerre, J. P.; Hayakawa, K.; Kwak, J. C. T. *Colloids Surf.* **1985**, *13*, 35.

- (22) Shirahama, K.; Musaki, T.; Takashima, K. In *Microdomains in Polymer Solutions*; Dubin, P., Ed.; Plenum: New York, 1985.
- (23) Li, Y.; Dubin, P. L. *ACS Symp. Ser.* **1994**, *578*, 320.
- (24) Antonietti, M.; Henke, S.; Thünemann, A. *Adv. Mater.* **1996**, *8*, 41.
- (25) Yasuda, H. *Plasma Polymerization*; Academic: London, 1985.

ion headgroup separated by an ethylene spacer from the fluorinated tail, structure 1) to well-defined acrylic acid



plasma polymer thin films has been investigated using XPS and contact angle analysis. Particular emphasis has been placed upon how these self-assembled polyelectrolyte-fluorosurfactant complexes differ in structure and liquid repellency compared to their conventional bulk analogues prepared in solution.

Experimental Section

Plasma polymerization experiments were performed in an electrodeless cylindrical glass reactor (5 cm diameter) enclosed in a Faraday cage.²⁷ The reactor was pumped by a two-stage rotary pump (Edwards E2M2) fitted with a liquid nitrogen cold trap (base pressure of 5×10^{-3} mbar). A 13.56 MHz radio frequency (rf) power source was coupled to a copper coil (10 turns) wound around the plasma chamber via an L-C matching unit. For pulsed plasma deposition experiments, a signal generator was used to trigger the rf power supply on the microsecond to millisecond time scale. The peak power (P_p), the plasma on-time (t_{on}), and off-time (t_{off}) could be varied independently. The overall average power input ($\langle P \rangle$) was calculated using the following equation:²⁸

$$\langle P \rangle = P_p \left| \frac{t_{\text{on}}}{t_{\text{on}} + t_{\text{off}}} \right| \quad (1)$$

Prior to each deposition, the reactor was scrubbed with detergent, rinsed with 2-propanol, oven dried, and further cleaned using a 50 W air plasma operating at a pressure of 0.2 mbar for 30 min. Glass substrate slides were washed in detergent, followed by ultrasonic degreasing in a 1:1 cyclohexane/2-propanol solvent mixture for 1 h. Acrylic acid (Aldrich 99%, further purified by multiple freeze-thaw cycles) was admitted into the reactor via a needle valve at a pressure of 0.2 mbar for 2 min prior to plasma ignition. Upon completion of deposition, the system was flushed with monomer for a further 2 min, and subsequently vented to air.

Acrylic acid plasma polymer coated glass slides were immediately immersed into a dilute solution of the cationic fluorosurfactant (Hoechst AG, Hoe L 3658-1), and then rinsed several times in water, prior to being dried in air.

The conventional complex was prepared by adding a 1% aqueous solution of poly(acrylic acid) to the surfactant until there was no further precipitation. The obtained gel was separated by filtration, and repeatedly washed with water. It was then redissolved in methanol and solvent cast to produce a film.

A Vacuum Generators ESCALAB Mk II system was used for XPS characterization of the coated glass slides. This was equipped with a nonmonochromatic X-ray photoexcitation source (Mg $K\alpha_{1,2} = 1253.6$ eV), and a concentric hemispherical analyzer (CHA) operating in constant analyzer energy mode (CAE; 20 eV pass energy). The emitted electrons were collected at a 30° takeoff angle from the substrate normal. The C(1s) hydrocarbon peak at 285.0 eV was chosen as a reference offset. Instrumentally determined sensitivity factors for unit stoichiometry were taken as C(1s):F(1s):O(1s):N(1s):Si(2p) = 1.00:0.24:0.39:0.65:0.97, respectively. A Marquardt minimization computer program was used to fit the XPS core level spectra

(26) Morosoff, N. *An Introduction to Plasma Polymerization*. In *Plasma Deposition, Treatment, and Etching*; d'Agostino, R., Ed.; Academic: London, 1990; p 1.

(27) Shard, A. G.; Munro, H. S.; Badyal, J. P. S. *Polym. Chem.* **1991**, *31*, 152.

(28) Bell, A. T.; Nakajima, K.; Shen, M. *J. Appl. Polym. Sci.* **1979**, *23*, 2627.

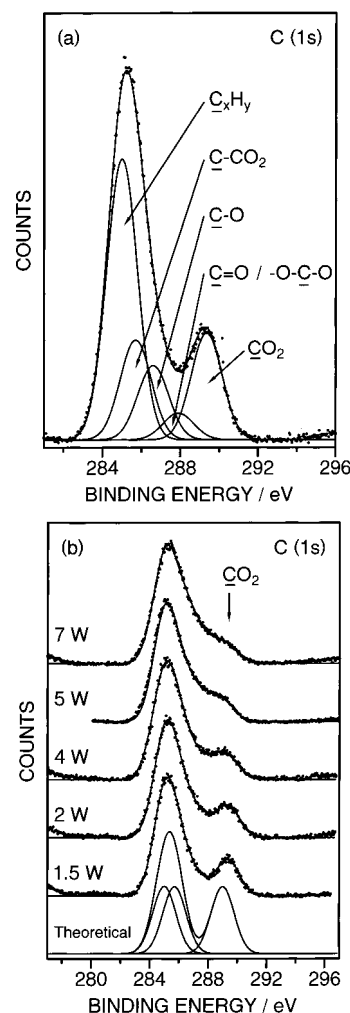


Figure 1. XPS C(1s) spectra: (a) peak fit for 2 W CW acrylic acid plasma polymer and (b) variation with CW power.

with fixed width Gaussian peak shapes.²⁹ The reported errors represent the combined statistical variation of peak fitting and experimental reproducibility. The absence of any Si(2p) XPS feature following plasma deposition was assumed to be indicative of complete coverage of the glass substrate.

Deposition rate measurements comprised measuring the change in mass of a quartz crystal sensor (Kronos QM300) positioned in the center of the plasma reactor, thereby providing in situ monitoring during the deposition process.

Sessile drop contact angle measurements were carried out using a video capture apparatus (A.S.T. Products VCA2500XE). High-purity water (hydrophobicity) and hexadecane (oleophobicity) were employed as the probe liquids.

Results

The C(1s) XPS envelope of a typical deposited acrylic acid plasma polymer layer could be fitted to five different carbon functionalities:³⁰ C_xH_y (285.0 eV), $\text{C}-\text{CO}_2$ (285.7 eV), $\text{C}-\text{O}$ (286.6 eV), $\text{O}-\text{C}-\text{O}/\text{C}=\text{O}$ (287.9 eV), and CO_2 (289.0 eV), Figure 1. Corresponding Mg $K\alpha_{3,4}$ satellite peaks were shifted by ~ 9 eV toward lower binding energy.³¹ The extent of carboxylate group (CO_2) incorporation into the plasma polymer was calculated

(29) Loh, F. C.; Tan, K. L.; Kang, E. T.; Kato, K.; Uyama, Y.; Ikada, Y. *Surf. Interface Anal.* **1996**, *24*, 597.

(30) Beamson, G.; Briggs, D. *High-Resolution XPS of Organic Polymers, The Scienta ESCA 300 Database*; John Wiley & Sons: Chichester, U.K., 1992.

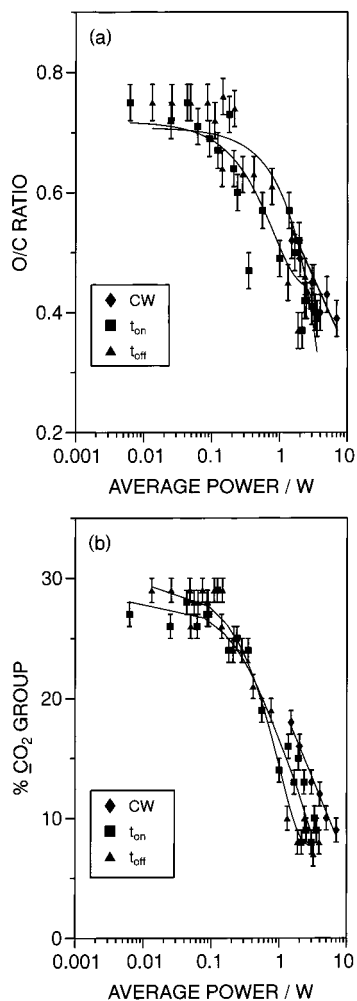


Figure 2. XPS data for CW versus pulsed plasma polymerization as a function of average power: (a) O/C ratio and (b) percent CO_2 group incorporation.

in terms of its percentage contribution to the overall C(1s) envelope. As reported in earlier continuous wave (CW) plasma polymerization studies of acrylic acid,^{25,32–35} oxygen incorporation and carboxylate group retention improved with decreasing power levels at the expense of other types of oxygenated functionalities and cross-linked sites, approaching O/C ratios as high as 0.52 ± 0.02 and carboxylate group retention of $18 \pm 1\%$, at 1.5 W, Figures 1 and 2. These values are considerably less than the expected theoretical O/C ratio of 0.67 and carboxylate group concentration of 33% anticipated from the acrylic acid monomer structure, $\text{CH}_2=\text{CHCO}_2\text{H}$.

Further improvement in structural retention was achieved by pulsing the electrical discharge. Low duty cycles (short on-periods or long off-times) enhanced oxygen and carboxylate group incorporation into the deposited plasma polymer structure, Figure 2. O/C

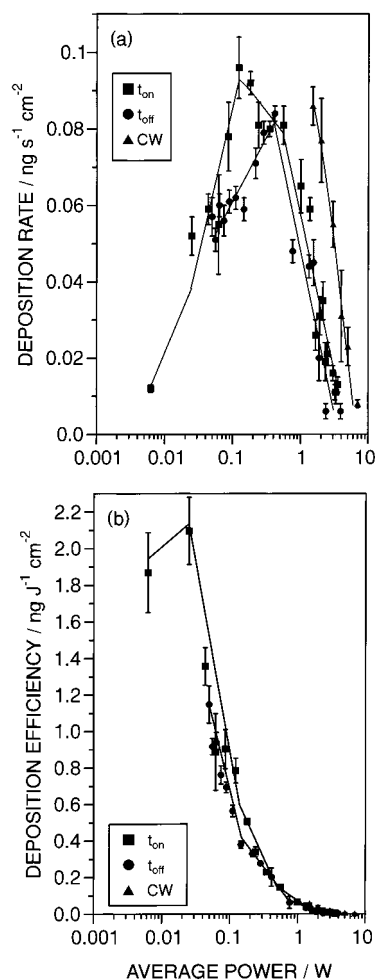


Figure 3. Plasma polymerization of acrylic acid: (a) deposition rate; and (b) deposition efficiency.

ratios as high as 0.72 ± 0.03 and carboxylate group concentrations of $30 \pm 1\%$ were attained by this method. These values are significantly better than what could be achieved during CW deposition. Eventually, at very short duty cycles, the glow discharge became unstable.

In situ quartz crystal monitoring revealed that the deposition rate increases with decreasing power during CW conditions, Figure 3. This observation is consistent with the detection of a Si(2p) signal from the glass substrate at powers greater than 7 W. Electrical pulsing extended this trend toward lower average powers, culminating in a maximum deposition rate of $0.1 \text{ ng s}^{-1} \text{cm}^{-2}$ at 0.1 W. Shorter duty cycles produced a fall in deposition rate. To factor out the variation in average power, the deposition rate per joule (deposition efficiency) is a useful parameter^{36–38} and was calculated using the following equation:³⁷

$$\text{deposition efficiency} = \frac{\text{deposition rate}}{\text{average power}} \quad (2)$$

In fact, the deposition efficiency improves with decreasing average power, indicating that film-forming reac-

(31) Briggs D.; Seah M. P. *Practical Surface Analysis by Auger and X-ray Photoelectron Spectroscopy*; John Wiley and Sons: Chichester, U.K., 1983.

(32) Yasuda, H.; Hsu, T. *J. Polym. Sci., Polym. Chem. Ed.* **1977**, *15*, 81.

(33) O'Toole, L.; Beck, A. J.; Ameen, A. P.; Jones, F. R.; Short, R. D. *J. Chem. Soc., Faraday Trans.* **1995**, *91*, 3907.

(34) Cho, D. L.; Claesson, P. M.; Gölander, C.-G.; Johansson, K. *J. Appl. Polym. Sci.* **1990**, *41*, 1373.

(35) Candan, S.; Beck, A. J.; O'Toole, L.; Short, R. D. *J. Vac. Sci. Technol., A* **1998**, *16*, 1702.

(36) Panchalingam, V.; Chen, X.; Savage, C. R.; Timmons, R. B.; Eberhart, C. *J. Appl. Polym. Sci., Appl. Polym. Symp.* **1994**, *54*, 123.

(37) Hynes, A. M.; Badyal, J. P. S. *Chem. Mater.* **1998**, *10*, 2177.

(38) Chen, X.; Rajeshwar, K.; Timmons, R. B.; Chen, J.-J.; Chyan, O. M. R. *Chem. Mater.* **1996**, *8*, 1067.

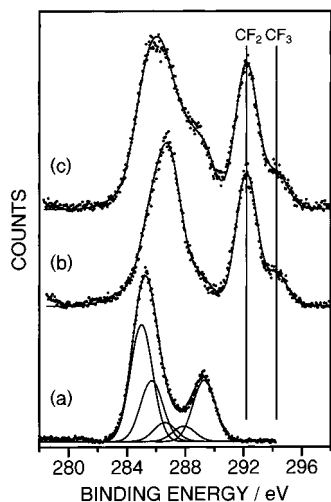


Figure 4. XPS C(1s) stack plot of (a) electrically pulsed acrylic acid plasma polymer ($t_{\text{on}} = 100 \mu\text{s}$, $t_{\text{off}} = 4 \text{ ms}$, $P_p = 5 \text{ W}$), (b) solvent cast poly(acrylic acid)–cationic fluorosurfactant complex, and (c) electrically pulsed acrylic acid plasma polymer ($t_{\text{on}} = 100 \mu\text{s}$, $t_{\text{off}} = 4 \text{ ms}$, $P_p = 5 \text{ W}$) reacted with cationic fluorosurfactant solution.

Table 1. C(1s) XPS Peak Fits

substrate	% Functionality	
	CF_2	CF_3
solvent cast bulk polyelectrolyte-surfactant complex	25 ± 1	6 ± 1
surfactant complexed to plasma polymer	29 ± 2	7 ± 1

Table 2. Probe Liquid Contact Angle Measurements

substrate	contact angle (deg) in two test liquids	
	water	hexadecane
surfactant-treated glass	38 ± 3	20 ± 3
solvent cast bulk polyelectrolyte-surfactant complex	120 ± 8	79 ± 3
surfactant complexed to plasma polymer	<20	82 ± 4

tions become progressively more dominant over film ablation and termination processes at lower powers,³⁶ Figure 3.

Pulsed plasma polymer coated glass slides containing a high surface concentration of carboxylic acid groups were immersed into a solution of cationic fluorinated surfactant and then rinsed several times in water. XPS analysis showed that a highly fluorinated surface was produced, which resembled the conventional poly(acrylic acid)–fluorosurfactant complex coating cast from methanol solution, Figure 4 and Table 1. However, whereas the latter displayed the expected water and oil repellency,³⁹ the fluorosurfactant–plasma polymer complex surface was found to switch between oleophobic and hydrophilic behavior, Table 2. XPS confirmed the absence of any I^- counterion belonging to the cationic fluorosurfactant being retained at the surface.

Discussion

Plasma polymers of acrylic acid have already found application in a wide range of surface-related phenom-

ena: control of substrate wettability,³⁴ protein adsorption,⁴⁰ modification of adhesion,⁴¹ interaction with biological species,⁴² and ultrafiltration.⁴³ In each case, control of carboxylic acid group density at the substrate surface is critical.

Improvement in structural retention of the carboxylic group seen with decreasing CW power (Figures 1 and 2) can be attributed to changes in the average electron energy, the electron energy distribution, and the density of excited species contained within the glow discharge.⁴⁴ Opening of the acrylic acid carbon–carbon double bond requires approximately 2.74 eV, whereas 3.61 eV is necessary for carbon–carbon single bond dissociation.³⁴ Therefore, a drop in the number of high-energy electrons in the electron energy distribution on moving toward lower average powers will favor polymerization reaction pathways in preference to monomer fragmentation or cross-linking processes.⁴⁵ Furthermore, this smaller proportion of high-energy electrons can be expected to reduce the degree of molecular excitation, and hence attenuate the extent of VUV damage of the growing polymeric film.⁴⁶ A corresponding drop in plasma sheath potential⁴⁵ should curtail ion-assisted cross-linking and substrate sputtering.⁴⁷ In addition, less monomer fragmentation at lower powers (carbon–oxygen single bond dissociation energy 3.64 eV and carbon–oxygen double bond dissociation energy 7.55 eV)⁴⁸ will help to minimize atomic oxygen-assisted chemical etching of the growing plasma polymer layer.⁴⁹

Pulsing the electrical discharge on the millisecond to microsecond time scale provides further improvement in carboxylic acid group retention due to milder VUV and ion-assisted damage, as well as conventional polymerization reaction pathways being allowed to proceed during the duty cycle off-period.^{25,32} Similar improvement in structural retention has been noted in the past for silicon-containing monomers,^{36,50,51} halocarbons,^{36,37,50,52,53} organometallic precursors,⁵⁴ alcohols,⁵⁵ epoxides,⁵⁶ and other reactive molecules.⁵⁷ The

(40) Lassen, B.; Malmsten, M. *J. Mater. Sci. Mater. Med.* **1994**, *5*, 662.

(41) Carlsson, C. M. G.; Johansson, K. S. *Surf. Interface Anal.* **1993**, *20*, 441.

(42) Ko, T. M.; Cooper, S. L. *J. Appl. Polym. Sci.* **1993**, *47*, 1601.

(43) Cho, D. L.; Ekengren, O. *J. Appl. Polym. Sci.* **1993**, *47*, 2125.

(44) McTaggart, F. K. *Plasma Chemistry in Electrical Discharges*; Elsevier: London, 1967.

(45) Grill, A. *Cold Plasmas in Materials Technology*; IEEE: Piscataway, NJ, 1994.

(46) Hudis, M.; Prescott, L. E. *Polym. Lett.* **1972**, *10*, 179.

(47) Flamm, D. L. Introduction to Plasma Chemistry. In *Plasma Etching: An Introduction*; Manos, D. M., Flamm, D. L., Eds.; Academic: London, 1989; p 91.

(48) Smith, E. B., *Basic Chemical Thermodynamics*, 4th ed.; Clarendon: Oxford, U.K., 1992.

(49) Cain, S. R.; Egitto, F. D.; Emmi, F. *J. Vac. Sci. Technol.* **1987**, *A5*, 1578.

(50) Panchalingam, V.; Chen, X.; Savage, C. R.; Timmons, R. B.; Huo, H.-H. *ASAIO J.* **1993**, *M305*.

(51) Anandan, C.; Mukherjee, C.; Seth, T.; Dixit, P. N.; Bhattacharyya, R. *Appl. Phys. Lett.* **1995**, *66*, 85.

(52) Ryan, M. E.; Hynes, A. M.; Badyal, J. P. S. *Chem. Mater.* **1996**, *8*, 37.

(53) Timmons, R. B.; Savage, C. R. *Chem. Mater.* **1991**, *3*, 575.

(54) Hashimoto, K.; Hikosaka, Y.; Hasegawa, A.; Nakamura, M. *Jpn. J. Appl. Phys.* **1996**, *35*, 3363.

(55) Rinsch, C. L.; Chen, X.; Panchalingam, V.; Eberhart, C.; Wang, J.-H.; Timmons, R. B. *Langmuir* **1996**, *12*, 2995.

(56) Tarducci, C.; Kinmond, E. J.; Brewer, S. A.; Willis, C.; Badyal, J. P. S. *Chem. Mater.*, in press.

(57) Uchida, T.; Senda, K.; Vinogradov, G. K.; Morita, S. *Thin Solid Films* **1996**, *281–282*, 536.

(39) Kissa, E. Repellent Finishes. In *Handbook of Fibre Science and Technology*; Part B.; Lewin, M., Sells, S. B., Eds.; Marcel Dekker: New York, 1984; p 143.

observed maximum in deposition rate measured during pulsed plasma polymerization corresponds to a situation where film ablation reactions are negligible, and conventional polymerization reactions proceed rapidly during the duty cycle off-period^{36,52} (i.e., minimal chemical etching by atomic oxygen, VUV and ion damage, or termination processes). The fall seen in deposition efficiency toward very low duty cycles can be attributed to the lack of a sufficient number of active species being created during the electrical discharge on-period necessary to sustain a significant rate of conventional polymerization processes.

These highly functionalized acrylic acid plasma polymer surfaces were found to readily undergo complexation with the cationic fluorosurfactant solution. A number of factors are known to govern the adsorption of surfactants onto solid surfaces: the chemical nature of the solid surface, the molecular structure of the surfactant, and the solvent environment.^{58–68} Surfactant adsorption at low concentrations normally involves single surfactant ions rather than micelles.^{1,69,70} Since carboxylic acid groups at the surface of the plasma polymer layer will become weakly ionized in water (the degree of ionization of poly(acrylic acid) in aqueous solution is 0.026),¹⁴ this will lead to a favorable electrostatic attraction between the ionized surface acid groups and oppositely charged fluorosurfactant ions.^{58,59} Such interactions will assist in orientating the charged surfactant headgroup toward the plasma polymer surface, and leave the fluorinated tail segment extended away toward the air–solid interface. The high contact angle measured for hexadecane is consistent with the aforementioned description, Table 2. However, the observed wettability toward water is indicative of a polar component at the surface, something which is absent for conventional bulk polyelectrolyte–surfactant complexes,²⁴ and also in the case of cationic fluorocarbon surfactant monolayers adsorbed onto negatively charged mica surfaces, where perfluoroalkyl chains remain orientated outward in the presence of both polar and nonpolar probe liquids.^{66,67} One possible explanation for the observed switching in liquid repellency could be that the adsorbed fluorosurfactant species form a partly

intercalated heterogeneous structure with some of the surfactant hydrophilic polar groups orientated away from the substrate (e.g., a bilayer).^{66,71,72,73,74,75} The driving force for such behavior would be a balance between attraction of the cationic surfactant headgroup toward the partially ionized polyelectrolyte surface and the unfavorable surface tension between the fluorocarbon tails and water.⁶⁶ However, this is unlikely due to the absence of any XPS signal from the I[−] counterion. A more plausible scenario is that the surfactant–polyelectrolyte monolayer is able to reorganize in such a way so as to allow water molecules to interact with the hydrophilic subsurface of the acrylic acid pulsed plasma polymer layer. Any plasma-induced cross-linking during deposition of the acrylic acid plasma polymer layer will restrict subsurface swelling, and therefore prevent accessibility for the fluorosurfactant moieties to below the surface; in turn this should suppress interdigitation, cooperative binding, and layering of the perfluoroalkyl tails.^{12,76} Such oleophobicity/hydrophilicity behavior is potentially attractive for antifogging applications, where the spreading of water droplets in combination with a hindrance toward oily substances is highly sought after.⁷⁷ Another area of interest is soil release, where the substrate is required to repel oily substances in the dry state while allowing solvent molecules access to the surface in the wet state, so as to allow the removal of any adhered soil moieties.^{78,79}

Complexing of other types of cationic fluorosurfactants to anionic pulsed plasma polymers prepared from acrylic acid and related monomers, e.g., 6-heptenoic acid, were also found to display similar liquid wetting behavior toward hexadecane and water (i.e., switching). This behavior extended to anionic fluorosurfactants complexed to cationic pulsed plasma polymer surfaces (e.g., allylamine monomer).

Conclusions

Complexation of ionic fluorosurfactants to polyelectrolyte plasma polymer surfaces gives rise to oleophobicity in combination with hydrophilicity. This “smart” behavior is found to be reversible and attributable to surface reconstruction phenomena.

Acknowledgment. We are grateful to DuPont and Hoechst for the generous gift of fluorosurfactant solutions.

CM000123I

(58) Rosen, M. J. *Surfactants and Interfacial Phenomena*, 2nd ed.; John Wiley & Sons: New York, 1989.

(59) Myers, D. *Surfactant Science and Technology*; VCH: New York, 1988.

(60) Lens, J. P.; Terlingen, J. A. C.; Engbers, G. H. M.; Feijen, J. *Langmuir* **1998**, *14*, 3214.

(61) Somasundaran, P.; Krishnakumar, S. *Colloids Surf., A* **1994**, *93*, 79.

(62) Biswas, S. C.; Chatteraj, D. K. *J. Colloid Interface Sci.* **1998**, *205*, 12.

(63) Esumi, K.; Iitaka, M.; Koide, Y. *J. Colloid Interface Sci.* **1998**, *208*, 178.

(64) Yamada, S.; Israelachvili, J. *J. Phys. Chem. B* **1998**, *102*, 234.

(65) Waltermo, Å.; Sjöberg, M.; Anhed, B.; Claesson, P. M. *J. Colloid Interface Sci.* **1993**, *156*, 365.

(66) Claesson, P. M.; Herder, P. C.; Berg, J. M.; Christenson, H. K. *J. Colloid Interface Sci.* **1990**, *136*, 541.

(67) Christenson, H. K.; Claesson, P. M.; Berg, J.; Herder, P. C. *J. Phys. Chem.* **1989**, *93*, 1472.

(68) Otsuka, H.; Esumi, K. *Langmuir* **1994**, *10*, 45.

(69) Kölbel, H.; Hörig, K. *Angew. Chem.* **1959**, *71*, 691.

(70) Kölbel, H.; Kuhn, P. *Angew. Chem.* **1959**, *71*, 211.

(71) McGuiggan, P. M.; Pashley, R. M. *Colloids Surf.* **1987**, *27*, 277.

(72) Pashley, R. M.; McGuiggan, P. M.; Horn, R. G.; Ninham, B. V. *J. Colloid Interface Sci.* **1988**, *126*, 569.

(73) Lai, C.-L.; Harwell, J. H.; O'Rear, E. A.; Komatsuzaki, S.; Arai, J.; Nakakawaji, T.; Ito, Y. *Colloids Surf., A* **1995**, *104*, 231.

(74) Lens, J. P.; Terlingen, J. A. C.; Engbers, G. H. M.; Feijen, J. *Langmuir* **1998**, *14*, 3214.

(75) *Cationic Surfactant Physical Chemistry*; Rubingh, D. N., Holland, P. M., Eds.; Surfactant Science Series Vol. 37; Marcel Dekker Inc.: New York, 1991.

(76) Ober, C. K.; Wegner, G. *Adv. Mater.* **1997**, *9*, 17.

(77) Ueno, M.; Ugajin, Y.; Horie, K.; Nishimura, T. *J. Appl. Polym. Sci.* **1990**, *39*, 967.

(78) Sherman, P. O.; Smith, S.; Johannessen, B. *Textile Res. J.* **1969**, *39*, 449.

(79) Ellzey, S. E.; Connick, W. J.; Drake, G. L.; Reeves, W. A. *Textile Res. J.* **1969**, *39*, 809.